Journal of Loss Prevention in the Process Industries 92 (2024) 105472

Contents lists available at ScienceDirect

Journal of Loss Prevention in the Process Industries

journal homepage: www.elsevier.com/locate/jlp

Enhancing safety in the storage of hazardous molecules: The case of hydroxylamine

Giuseppe Andriani [a], Paolo Mocellin [a,b], Gianmaria Pio [c], Chiara Vianello [a,b], Ernesto Salzano [c,*]

[a] Università Degli Studi di Padova. Dipartimento di Ingegneria Industriale, Padova, Italy
[b] Università Degli Studi di Padova. Dipartimento di Ingegneria Civile, Edile e Ambientale, Padova, Italy
[c] Università di Bologna. Dipartimento di Ingegneria Civile, Chimica, Ambientale e Dei Materiali, Bologna, Italy

ARTICLE INFO

Keywords:
Storage vessels
Process safety
Stability diagrams
Thermal decompositions
Runaway reactions

ABSTRACT

Handling large quantities of thermally unstable compounds in storage vessels can result in severe accidents due to runaway reactions. Therefore, developing inherently safe design strategies for storage equipment is crucial for enhancing chemical plant reliability and preventing hazardous scenarios. The Frank-Kamenetskii theory (FKT) of self-heating offers practical tools for designing procedures to address phenomena that could lead to uncontrolled chemical reactions. This study introduces a design procedure based on the FKT for creating intrinsically safe storage vessels. An expanded FKT version incorporating parametric sensitivity analysis has been developed to improve the method's reliability. To understand self-heating phenomena, stability and performance diagrams were created, relating critical design parameters (e.g., the critical value of the Frank-Kamenetskii number) and verification parameters (e.g., maximum reached dimensionless temperature) to the dimensionless activation energy (γ). Additionally, the proposed design strategy includes a procedure for designing relief systems to mitigate the risk of equipment explosions from runaway reactions. The applicability of this procedure was tested using two cases: (I) an aqueous solution containing 50% w/w hydroxylamine (HA) and (II) a 50% w/w HA aqueous solution with 1% w/w hydroxylamine hydrochloride (HA-derived salt). Results indicate that for large γ values, the traditional FKT formulation and the expanded theory yield similar vessel designs. However, for finite γ values ($\gamma \leq 100$), the refined FKT version allows for less conservative storage equipment design. Combining DIERS guidelines with standard procedures for relief systems results in a more versatile and consistent protocol. However, incorporating relief systems is often impractical for large storage vessels due to the excessively large venting areas required for runaway reactions. In such cases, intrinsically safe vessel designs become the only feasible solution to prevent catastrophic incidents.

Nomenclature

A_{gas}	Gas orifice area (DIERS method)
A_{vap}	Vapour orifice area (DIERS method)
A_{tot}^{DIERS}	Total orifice (DIERS method)
A_{tot}^{std}	Total orifice area (standard method)
ARSST™	Advanced reactive system screening tool
Bi	Biot number
C	Fluid flow coefficient
C_{A0}	Initial molar concentration of the reactant A
$\widetilde{C}_p$	Heat capacity per unit moles of the liquid
$\widehat{C}_p$	Heat capacity per unit mass of the liquid
$\widetilde{C}_{p,w}$	Heat capacity per unit moles of water
D	System diameter
d	Diameters ratio
D_{valve}	Valve diameter under the assumption of circular orifice
DIERS	Design Institute for Emergency Relief Systems
E_a	Apparent activation energy
FKT	Frank-Kamenetskii theory of self-hating
H	System height
H/D	Aspect ratio
HA	Hydroxylamine
K_b	Backpressure coefficient
K_c	Combination factor coefficient
K_d	Discharge coefficient
$k_{k\infty}$	Apparent Arrhenius pre-exponential factor
k_T	Thermal conductivity of the liquid mixture
$k_{T,w}$	Thermal conductivity of water

(*continued on next column*)

(*continued*)

(*continued on next page*)

* Corresponding author.
E-mail address: ernesto.salzano@unibo.it (E. Salzano).

https://doi.org/10.1016/j.jlp.2024.105472
Received 28 August 2024; Received in revised form 24 October 2024; Accepted 25 October 2024
Available online 6 November 2024

(*continued*)

m_{tot}	Initial reactive mass in the test apparatus
n	Apparent reaction order
$\dot{P}_{peak}$	Temporal pressure rate at peak conditions
P_{onset}	Onset pressure
P_{relief}	Relief pressure
PM	Molecular weight of mixture
PM_{gas}	Molecular weight of gas
PM_{vap}	Molecular weight of vapour
PM_w	Molecular weight of water
QRA	Quantitative risk assessment
R_g	Universal gas constant
$\mathscr{R}\|_{T_w,C_{A0}}$	Reaction rate at wall temperature
r_w	System radius
$S(\Theta;\delta)$	Normalized sensitivity of Θ to the respect of δ
$\mathscr{T}$	Dimensionless time
T_{center}	Temperature in the centre of the system
T_{max}	Maximum system's temperature
T_{onset}	Onset temperature
$\dot{T}_{onset}$	Temporal temperature rate at onset conditions
T_{relief}	Relief temperature
$\dot{T}_{relief}$	Temporal temperature rate at relief conditions
T_w	Wall temperature
t_{cond}	Characteristic time for heat conduction
TRA	Thermal risk assessment
TS^U	Thermal screening unit
V	System volume
V_{gas}^{test}	Gas volume in the test apparatus
VMWT	Varma, Morbidelli and Wu theory
VSP2™	Vent size package 2
$\dot{W}_{gas}$	Gas required relief mass flow rate
Greek symbols	
α_0	Void fraction
$\widehat{\lambda}$	Heat of vaporization of the mixture per unit mass
γ	Dimensionless activation energy
ρ	Liquid mixture density
$\Delta\widetilde{H}_r$	Molar enthalpy of reaction
ρ_{gas}	Gas density measured at relief conditions
δ	Frank-Kamenetskii number
ρ_w	Water density
δ_{crit}	Critical Frank-Kamenetskii number
χ	Main reactant conversion
Θ	Dimensionless temperature
Ω	Dimensionless radial coordinate
Θ_{max}	Maximum value of the dimensionless temperature

1. Introduction

Exothermic thermal decomposition reactions pose significant concerns due to the potential for runaway reactions (Mocellin et al., 2022). The Health and Safety Executive reported 189 accidents caused by runaway reactions between 1962 and 1987 (Barton and Nolan, 1991). From 1988 to 2013, Saada et al. documented an additional 30 accidents in the UK, primarily using data from the FACTS database and other literature sources (Saada et al., 2015). According to the ARIA database, in the last decade, 14 accidents due to uncontrolled exothermic reactions occurred in France (ARIA). In China, from 1984 to 2019, there were 271 industrial accidents caused by runaway reactions, consistent with the reported data for the French industry (Zhang et al., 2021; Dakkoune et al., 2019). In the USA, the CSB database recorded 13 industrial accidents under the "reactive incident" category from 2000 to 2023 (CSB database). Two notorious industrial accidents related to runaway reactions are the Bhopal disaster (December 3, 1984) and the Seveso disaster (July 10, 1976). The Bhopal accident involved an uncontrolled chemical reaction of methyl isocyanate under storage conditions (Yang et al., 2015; Eckerman, 2005), while the Seveso accident was caused by a runaway reaction inside a chemical reactor due to system malfunction (Fabiano et al., 2017; Jain et al., 2017). Both incidents had devastating consequences, resulting in thousands of deaths and the release of toxic substances that caused long-term environmental and health impacts.

Runaway reactions are typically associated with uncontrolled heat management within the system (Andriani et al., 2024c). When an exothermic chemical reaction generates thermal energy, the system's temperature will rise if heat is not effectively dissipated from the reactive mixture (Vianello et al., 2018a). The reaction rate of chemical reactions depends exponentially on temperature, and the thermal power generated by a chemical process is a function of the reaction rate and enthalpy. This creates a feedback loop where an increase in temperature leads to an increased reaction rate, generating more heat. Once a runaway loop is triggered, the rapid temperature rise can cause fluid volatilisation and the formation of gaseous by-products due to additional unwanted chemical reactions. The generated vapours and gases, combined with the high temperature, can result in uncontrolled pressurisation of the system, potentially leading to explosions and the release of hazardous substances (Vianello et al., 2016). Fig. 1 graphically summarises the described runaway positive feedback mechanism.

Therefore, understanding the dynamics of decomposition reactions is crucial (Deng et al., 2016). Both experimental and numerical approaches can be adopted to achieve this understanding. Typically, experimental studies rely on calorimetric analysis (Pio et al., 2021) to quantify apparent reaction kinetics, thermodynamic properties, and onset and peak features (Vianello et al., 2018b). The data acquired from these studies are commonly used for quantitative risk assessment (QRA) (Juncheng et al., 2020), thermal risk assessment (TRA) (Wang et al., 2009), reactor design and control (Varma et al., 1999; Strozzi et al., 1999) or process development (Ozawa, 2000). However, unexpected hazardous scenarios can also arise during storage due to self-heating (Guo et al., 2013; Shanley, 1953). Therefore, the ideal approach is to design storage vessels according to the inherent safety paradigm (Kletz and Amyotte, 2010), considering the self-heating phenomenon to prevent accidental runaway reactions of the stored material.

From a numerical perspective, the Frank-Kamenetskii theory of self-heating (FKT) is commonly employed to investigate the behaviour of spontaneous self-heating phenomena that can potentially lead to hazardous scenarios (Frank-Kamenetskii, 1955). The FKT complements the Semenov theory of thermal explosion and is based on the hypothesis of a quiescent fluid contained in a system with negligible wall thermal resistance, represented by $Bi \to \infty$ (Boddington et al., 1983). Additionally, the theory assumes $\chi \to 0$ and an almost infinite dimensionless activation energy, defined as $\gamma = E_a/R_g T_w$. The FKT allows for the design of storage systems to prevent ignition or explosion (Babrauskas, 2003). For liquids, the assumption of a stored quiescent fluid is legitimate since, even if temperature gradients can induce natural convection, the average fluid velocity is practically zero (Campbell, 2015). Additionally, the vessel design will be conservative because natural convection, even if minimal, will help dissipate heat (Novozhilov, 2017; Lazarovici et al., 2005).

Considering a conductive static fluid, assuming $Bi \to \infty$ can be easily verified without compromising the modelling outcomes. Moreover, the

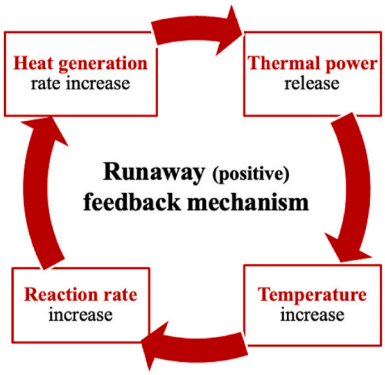

Fig. 1. Graphical representation of the positive feedback loop underlying runaway phenomena.

hypothesis of $\chi \to 0$ is realistic because the storage vessel must be designed to prevent the stored material from undergoing a fully developed decomposition reaction, allowing only negligible consumption due to collateral effects. However, the assumption that $\gamma \to \infty$ could lead to misleading conclusions, as it would only be verified for $E_a \to \infty$ or $T_w \to 0$. The former scenario is unphysical, while the latter involves temperatures not achievable in standard industrial practice during conventional storage. Therefore, it is better to investigate the dependence of the modelling outcomes on the values of γ to avoid misleading conclusions.

To overcome the limitations in the applicability of the Frank-Kamenetskii theory (FKT), it is recommended to expand the theory by considering the effect of γ on the primary variable involved in the storage vessel design: the critical value of the Frank-Kamenetskii number (δ_{crit}). The δ_{crit} is a meta-stable value above which a steady-state solution for a particular system becomes can not be reached due to runaway phenomena. The idea is to retrieve the δ_{crit} for a series of γ values through a sensitivity analysis (Andriani et al., 2024a).

In this context, the sensitivity analysis is analogous to applying bifurcation theory to a chemically reactive system (Lengyel and West, 2018). Specifically, the δ_{crit} value can be defined as a system meta-stable parameter above which the system's behavior shifts from stable to unstable. A $\delta - \gamma$ stability diagram will illustrate the functional dependence of δ_{crit} on γ, showing a safe-to-runaway transition curve. Below this limit curve, it is possible to identify parameter combinations that allow the stable storage of the material, whereas, above the curve, parameter combinations may trigger a runaway scenario. Ultimately, the $\delta - \gamma$ stability diagram can be used to assess, for a particular value of γ, the δ_{crit} number, enabling a more refined and safe storage vessel design.

Even though inherent safety is fundamental for correct design, passive and active protective items can be added to the equipment to keep hazards under control (Kletz, 2003). Specifically, relief devices can help avoid explosions and reduce potential losses related to runaway reactions (Singh, 1994). Since reactors and storage vessels are the most common equipment in accidents (Ho et al., 1998), adequately sized relief systems are strongly recommended.

In light of these considerations, the present work proposes a reproducible methodology for the intrinsically safe design of storage vessels containing thermally unstable components. Stability diagrams will be produced and used to support the design procedure (Pio and Salzano, 2020). To test the reliability of the proposed strategy, the procedure will be applied to the case of a 50% w/w aqueous solution of hydroxylamine (HA) and a 50% w/w HA solution containing an additional 1% w/w of hydroxylamine hydrochloride (HH), which have been experimentally investigated in previous studies (Andriani et al., 2024d). By comparing the HA aqueous solution with the HA-derived salt solution, it will be possible to quantify the effect of salt addition on the thermal stability of HA.

2. Materials and methods

Fig. 2 outlines the logical workflow of the proposed methodology.

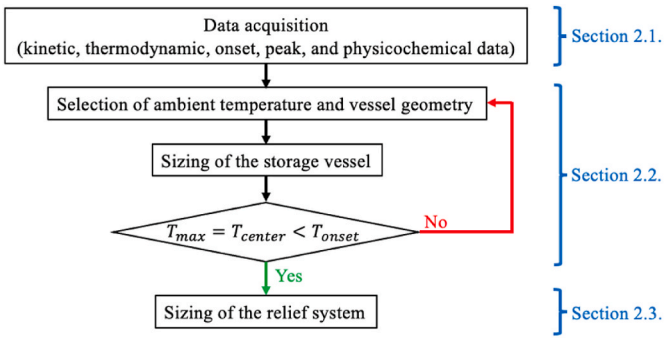

Fig. 2. Logical workflow of the proposed methodology.

The following sections will elucidate each step presented in Fig. 2. More specifically, in Section 2.1. The list of data needed for further implementation of the proposed sizing method of storage vessels and relief systems, handling liquid materials prone to decomposition reactions, is reported. Then, in Section 2.2. The methodology for storage vessel sizing is illustrated, involving the use of the original FKT or information retrieved from the $\delta - \gamma$ stability diagram. This diagram improves upon the FKT by incorporating sensitivity analysis. In Section 2.3, the procedure for the sizing of the relief system is elucidated. Eventually, in Section 2.4., the data required to apply the proposed procedure to the case study of the two mentioned hydroxylamine aqueous solutions will be provided.

2.1. Data acquisition

As illustrated in Fig. 2, the first step of the proposed methodology is to acquire the numerical values of the main constitutive variables. The input data set includes kinetic, thermodynamic, onset, peak, and physicochemical information.

- Kinetic data: Activation energy (E_a), pre-exponential factor ($k_{k\infty}$), reaction order (n), and initial concentration (C_{A0}).
- Thermodynamic data: Enthalpy change of the reaction ($\Delta\widetilde{H}_r$).
- Onset data: Onset temperature (T_{onset}), onset temperature rate ($\dot{T}_{onset}$),.
- Peak data: Peak pressure rate ($\dot{P}_{peak}$).
- Physicochemical data: Heat capacity ($\widetilde{C}_p$), thermal conductivity (k_T).

These quantities can be determined experimentally (Vianello et al., 2015) or obtained from literature correlations. For clarity, the list of symbols is provided in the Nomenclature Section. For completeness, it is essential to note that additional data obtainable through calorimetric screening include the onset pressure and pressure rate, as well as the maximum temperature, pressure, and pressure rate registered during the thermal analysis. This supplementary information is crucial for a thorough stability assessment of the decomposing substance under investigation.

2.2. Sizing of the storage vessel

The governing equation used to size the storage vessel is reported in Eq. (1) (Restuccia et al., 2017; Andriani et al., 2024b) based on the definition of the Frank-Kamenetskii number. For this analysis, the ambient temperature is assumed to be equal to T_w, due to the assumption of negligible thermal resistance of the wall. Three different ambient temperatures will be considered: 5 °C, 20 °C and 35 °C. The system geometry is considered as a vertically oriented cylindrical storage vessel. Consequently, a critical Frank-Kamenetskii number, δ_{crit}, of 2.00 is assumed, consistent with the original FKT (Balakrishnan and Wake, 1996), and invariant with γ. The maximum temperature reached in the bulk of the storage vessel will be verified to ensure it remains below the onset temperature (T_{onset}) to avoid decomposition. This verification step can be performed using Eq. (2) (Chambré, 1952), which is derived from the definition of the dimensionless in the FKT (Eq. (4)), and the maximum dimensionless temperature value reached for $\delta = \delta_{crit}$ (i.e., $\Theta_{max} = \ln 4$).

$$r_{w,crit} = \sqrt{\frac{\delta_{crit}\, k_T\, R_g\, T_w^2}{(-\Delta\widetilde{H}_r)\, \mathscr{R}|_{T_w,C_{A0}}\, E_a}} = \sqrt{\frac{\delta_{crit}\, k_T\, R_g\, T_w^2}{(-\Delta\widetilde{H}_r)\, k_{k\infty} \exp\left(-\frac{E_a}{R_g T_w}\right) C_{A0}^n\, E_a}} \tag{1}$$

$$T_{center} = T_w + \frac{R_g\, T_w^2}{E_a} \ln 4 < T_{onset} \tag{2}$$

The volume V of the storage vessel can be calculated while keeping

the height-to-diameter ratio (H/D) constant. This ratio significantly depends on the seismic zone where the tank is located (Myers, 1997), typically ranging from 0.5 to 2.4, or can be adjusted to limit mechanical integrity issues (Godoy, 2016) and space oppation (Gangloff et al., 2017). Additionally, a unique value of the coefficient α_0 can not be consistently retrieved in the literature (Geyer and Wisuri, 2000) because it varies depending on the application. Thus, the effect of varying these two parameters will be considered and discussed.

To determine the dependence of δ_{crit} on γ, the dimensionless transient heat balance equation for a conductive quiescent fluid, under the assumption of negligible conversion, must be considered. By performing a sensitivity analysis, the δ_{crit} related to a specific γ can be found as the characteristic value that maximises the normalized sensitivity $S(\Theta;\delta)$ at the centre of the system (i.e., $\Omega = 0$) at steady-state (i.e., $\mathscr{T} \to \infty$). The results of the sensitivity analysis can be presented in a $\delta - \gamma$ stability diagram, highlighting the functional dependence of δ_{crit} on γ with a safe-to-runaway transition curve. For each $\delta > \delta_{crit}$, the system exhibits unstable behaviour due to the onset of a runaway condition triggered by uncontrollable self-heating, making a steady state unreachable. For $\delta < \delta_{crit}$, the system can operate safely, reaching a stable, steady state. To ensure that $T_{center} < T_{onset}$, the Θ_{max} value will be reported for each δ_{crit} value. Table 1 summarises the various equilibrium characteristics, operational regimes and temperature check requirement for different δ values. It is important to note that the obtained parameters map will generally apply to any reactive system for which a storage vessel is being designed.

2.3. Constitutive model

In Eq. (3), the transient heat balance equation is used to determine the $\delta - \gamma$ stability diagram for a quiescent conductive fluid undergoing a negligible conversion decomposition reaction. This equation incorporates various dimensionless parameters, including Θ, γ, $\mathscr{T}$, δ and Ω. Due to the idealised cylindrical symmetry of the system, the spatial dependency of Θ is considered mono-dimensional, dependent only on $\Omega = r/r_w$. The meanings of these dimensionless parameters are detailed in Eqs. (4)–(7). Additionally, $\mathscr{T}$ depends on t_{cond}, defined as the ratio between the square radius of the system r_w^2 and the heat diffusivity $\alpha = k_T/\rho\widehat{C}_p$, as shown in Eq. (8). The sensitivity equation involved in the analysis is presented in Eq. (9). The expression for the sensitivity of Θ with respect to δ is given in Eq. (10), and the expression of $S(\Theta;\delta)$ is provided in Eq. (11).

$$\frac{\partial\Theta}{\partial\mathscr{T}} = \frac{\partial^2\Theta}{\partial\Omega^2} + \frac{1}{\Omega}\frac{\partial\Theta}{\partial\Omega} + \delta\exp\left(\frac{\Theta}{1+\Theta/\gamma}\right) \tag{3}$$

$$\Theta = \gamma\frac{T - T_w}{T_w} \tag{4}$$

$$\gamma = \frac{E_a}{R_g T_w} \tag{5}$$

$$\delta = \frac{\gamma\,\widetilde{Q}_r\,\mathscr{R}|_{T_w,C_{A0}}\,r_w^2}{k_T\,T_w} \tag{6}$$

$$\mathscr{T} = \frac{t}{t_{cond}} \tag{7}$$

$$t_{cond} = \frac{r_w^2}{\alpha} \tag{8}$$

$$\frac{\partial s(\Theta;\delta)}{\partial\mathscr{T}} = \frac{1}{\Omega}\frac{\partial}{\partial\Omega}\left[\Omega\frac{\partial s(\Theta;\delta)}{\partial\Omega}\right] + \exp\left(\frac{\Theta}{1+\Theta/\gamma}\right)\left[1 + \frac{\delta s(\Theta;\delta)}{(1+\Theta/\gamma)^2}\right] \tag{9}$$

$$s(\Theta;\delta) = \frac{\partial\Theta}{\partial\delta} \tag{10}$$

$$S(\Theta;\delta) = \frac{\delta}{\Theta}\frac{\partial\Theta}{\partial\delta} \tag{11}$$

Table 1
Equilibrium characteristics, operational regimes, and temperature check requirements as functions of different Frank-Kamenetskii number values.

	Thermal equilibrium	Regime	Check on $\mathbf{T}_{center}$
$\delta < \delta_{crit}$	Stable	Safe	Not required
$\delta = \delta_{crit}$	Metastable	Transitional	Not required
$\delta > \delta_{crit}$	Unstable	Runaway	Required

2.4. Relief system sizing

The first step of the relief device sizing procedure involves determining the orifice size and the flow rate of the discharged stream. For runaway gasses and vapour venting, it is recommended to follow the technique developed by the Design Institute for Emergency Relief Systems (DIERS) (Green and Southard, 2019). DIERS, under the auspice of AIChE, has significantly advanced the understanding of venting technology, especially for runaway reactions (Fisher et al., 1992). Applying the DIERS procedure for relief system design in the presence of a runaway reaction is also strongly recommended by API 521 (ANSI/API, 2007; API 2000; API, 1998). The design equations are reported in Eqs. (12) and (13). This work obtained information for implementing the method equations from a TS^{U} calorimeter instead of an ARSST™ coupled with a VSP2™. Corrections for the effects of cell instrument thermal inertia and heating rate of the oven were included to avoid inaccuracies and ensure data accuracy.

$$\dot{W}_{tot} = \dot{W}_{vap} + \dot{W}_{gas} = \frac{V(1-\alpha_0)\rho\widehat{C}_p\dot{T}_{relief}}{\widehat{\lambda}} + \frac{V(1-\alpha_0)\rho V_{gas}^{test}\dot{P}_{peak}\rho_{gas}}{m_{tot}P_{relief}} \tag{12}$$

$$A_{tot}^{DIERS} = A_{vap} + A_{gas} = \frac{V(1-\alpha_0)\rho\widehat{C}_p\dot{T}_{relief}}{0.61K_d\lambda P_{relief}}\left(\frac{R_g T_{relief}}{PM_{vap}}\right)^{0.5} + \frac{V(1-\alpha_0)\rho V_{gas}^{test}\dot{P}_{peak}}{0.61K_d m_{tot}P_{relief}}\left(\frac{PM_{gas}}{R_g T_{relief}}\right)^{0.5} \tag{13}$$

Eqs. (12) and (13) assume a two-phase vapour and gas flow, representing a hybrid venting system. The vapour phase forms due to the tempering of the reaction via the vaporization of the liquid phase, while the gaseous phase results from the decomposition of unstable materials. To test the reliability of the proposed sizing procedure, it will be compared to standard safety relief valve (SRV) design methods (Emerson, 2012; Hellemans, 2009). Traditional algorithms require the total mass flow rate $\dot{W}_{tot}$ to be known in advance, and specific correlations for runaway reactions are typically absent. The strength of the proposed methodology lies in its detailed consideration of valve functionalities, incorporating two additional coefficients apart from K_d: the backpressure correction factor for gasses and the K_c combination factor for installations with a rupture disc upstream of the valve. The design equation is presented in Eq. (14), assuming churn turbulent flow with an associated coefficient $C = 3.5 \bullet 10^{-3}$. All quantities must be expressed in SI units, and relief conditions are supposed to be equal to the onset conditions.

$$A_{tot}^{std} = \frac{3600\;W_{tot}}{2.39\;10^{-5}P_{relief}K_dK_bK_c}\sqrt{\frac{T_{relief}Z}{PM}} \tag{14}$$

2.5. Case study

The acquisition of the main physical and chemical data represents the primary input of the procedure schematically shown in Fig. 2. The

kinetic (E_a, $k_{k\infty}$, n, C_{A0}), thermodynamic ($\Delta\widetilde{H}_r$), onset (T_{onset}; $\dot{T}_{onset}$) and peak ($\dot{P}_{peak}$) data for 50 %w aqueous solution of HA and 50 %w of HA added with 1 %w of HH were retrieved from the work of (Andriani et al., 2024d). The dataset has been corrected to account for the thermal inertia of the instrument cell and the effect of the oven heating rate. The numerical values are reported in Table 2. The remaining physical properties can be calculated via established correlations. The $\widetilde{C}_p$ has been determined following the methodology reported in the literature (Andriani et al., 2024d). For k_T, the Predvoditelev correlation (Ozbek and Phillips, 1980) has been adopted (Eq. (15)).

$$k_T = k_{T,w}\frac{\widetilde{C}_p}{\widetilde{C}_{p,w}}\left(\frac{\rho}{\rho_w}\right)^{4/3}\left(\frac{PM_w}{PM}\right)^{1/3} \tag{15}$$

3. Results and discussions

This section first illustrates the $\delta-\gamma$ stability diagram (Section 3.1.). Then, Section 3.2. presents and critically discusses the outcomes of the sizing of the storage vessels. Finally, Section 3.3. elucidates and comments on the results obtained from implementing the relief system sizing, as detailed in Section 2.3.

3.1. $\delta-\gamma$ stability diagram

The $\delta-\gamma$ stability diagram has been determined following the procedure outlined in Section 2.2. The resulting parameter map is generally applicable to the design of any cylindrical storage vessel handling liquids prone to decomposition reactions, which can trigger self-heating phenomena, potentially leading to runaway conditions. Before discussing how to apply this information to design inherent safe storage vessels, the parameter map is presented in Fig. 3.

As observed in Fig. 3, the δ_{crit} value depends on the specific value of γ. An interesting feature of this trend is that as γ increases, δ_{crit} asymptotically approaches the value predicted by Frank-Kamenetskii under the approximation of $\gamma\to\infty$ (i.e., $\delta_{crit}=2$). This agreement between the results from the original FKT and those obtained in this work using an expanded FKT coupled with the VMWT serves as an initial validation of the modelling outcomes. From a practical perspective, knowing the exact value of γ in advance allows for a more reliable design of storage vessels, as it enables the use of a less approximated δ_{crit} value. Indeed, for low γ values, the actual δ_{crit} value deviates significantly from the asymptotic one, highlighting the importance of accurate parameter determination for effective vessel design.

To deeply understand the behaviour of a system modelled with the proposed expanded version of the FKT, it is worth analysing how Θ_{max} varies with γ for $\delta=\delta_{crit}$ and for $\delta=2$. This analysis emphasizes the consequences of selecting different δ_{crit} values during the design phase. The Θ_{max} can be used to retrieve the T_{max} value, which is crucial for verifying the onset temperature, as detailed in Section 2.2. Ensuring $T_{max}<T_{onset}$ indicates that the system has been designed to minimise the risk of runaway conditions triggered by the thermal decomposition of the stored material.

Examining the trend in Fig. 4, we observe excellent agreement between the outcomes of the proposed expanded FKT and its original version. As γ increases, the Θ_{max} values determined for both $\delta=\delta_{crit}$ and $\delta=2$ asymptotically approach the value predicted by the original FKT (i.e., $\Theta_{max}=\ln 4$). Designing a storage vessel with a constant $\delta_{crit}=2$, regardless of γ, results in a more conservative system at lower γ values. The difference between δ_{crit} values obtained with the expanded and original FKT increases as γ decreases, causing the difference between Θ_{max} values for $\delta=\delta_{crit}$ and $\delta=2$ to follow the same trend. As the distance between δ_{crit} and the constant value of 2 imposed by the FKT decreases, the system becomes more stable, reducing the magnitude of the self-heating phenomenon. Consequently, the achievable Θ_{max} decreases. Using a refined δ_{crit} value allows for designing a less conservative system compared to one designed with the constant value of δ_{crit} from the original FKT. This less conservative system can be envisioned with a

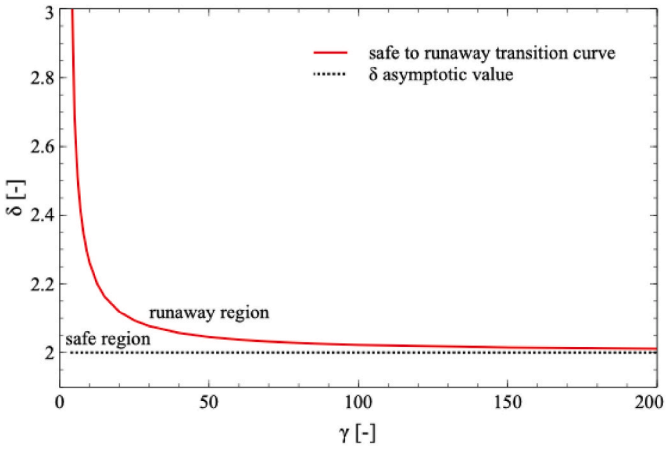

Fig. 3. $\delta-\gamma$ stability diagram. The red curve represents the safe-to-runaway transition boundaries, with the safe region below the curve and the runaway region above it. The dotted line indicates the asymptotic value of the Frank-Kamenetskii number, as determined by the original version of the self-heating theory. (For interpretation of the references to colour in this figure legend, the reader is referred to the Web version of this article.)

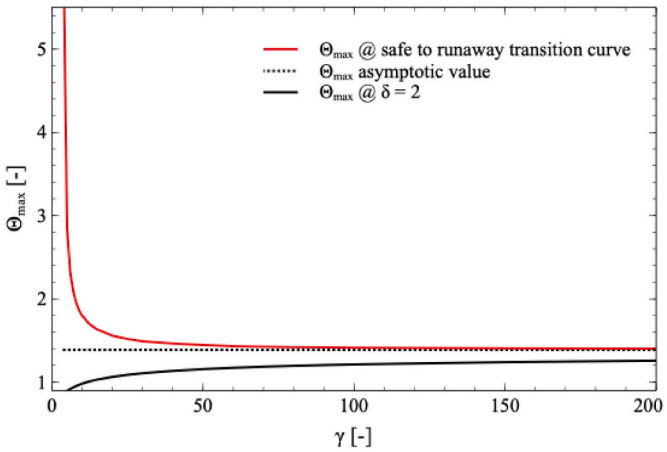

Fig. 4. Trend of the Θ_{max} as a function of γ. The red curve shows the trend of Θ_{max} determined for δ related to the safe-to-runaway transition boundary. The black curve shows the trend of Θ_{max} determined for $\delta=2$. The dotted line represents the asymptotic value of Θ_{max} as determined by tge original FKT. (For interpretation of the references to colour in this figure legend, the reader is referred to the Web version of this article.)

Table 2
Required variables for method implementation.

	E_a	$k_{k\infty}$	n	C_{A0}	$\Delta\widetilde{H}_r$	T_{onset}	$\dot{P}_{peak}$	$\dot{T}_{onset}$
	kJ mol^{-1}	s^{-1}	–	kmol m^{-3}	kJ mol	K	Pa s^{-1}	K s^{-1}
50 %wHA	103	$9.33\cdot10^{9}$	1	16.56	−79.8	393.15	$6.85\cdot10^{4}$	$6.26\cdot10^{-3}$
50 %wHA+1 %wHH	117	$6.51\cdot10^{10}$	1	17.82	−78.1	392.15	$6.85\cdot10^{4}$	$6.90\cdot10^{-3}$

larger vessel critical diameter, according to Eq. (2), still avoiding the onset of runaway conditions. A storage tank with a larger critical diameter can handle more reactive chemicals safely, given a constant aspect ratio. However, for tanks designed with the refined δ_{crit} value, checking T_{center} becomes more critical because the extent of the self-heating phenomenon will increase, as shown by the trend in Fig. 4. Using a refined δ_{crit} value necessitates verifying $T_{max} < T_{onset}$ with the appropriate Θ_{max} value to avoid potential runaway conditions. If the condition $T_{max} < T_{onset}$ is not satisfied, the adopted δ value must be decreased for a specific γ to ensure safe and reliable storage. A practical application of the $\delta - \gamma$ stability diagram and the $\Theta_{max} - \delta$ diagram will be presented in Section 3.2.

3.2. Sizing of the storage vessel

As described in Section 2.2, three atmospheric temperatures were considered: 5 °C, 20 °C and 35 °C. For clarity, the atmospheric, external, and internal vessel wall temperatures are identical due to the assumption of $Bi \to \infty$ and negligible thermal resistance of the equipment wall. Consequently, any change in atmospheric temperature will result in corresponding changes in the external and internal temperature walls. Tanks vessel has been calculated and is reported in Table 3. For comparison, the δ_{crit} and Θ_{max} values have been obtained from both the original and expanded FKT models.

As observed in Table 3, the external temperature significantly affects the critical radius of the system. The characteristic size of the vessel decreases markedly as the input temperature increases. This trend is consistent with the outcomes derived from the original and expanded versions of the FKT. To ensure the most reliable protection for a hypothetical plant, retrieving temperature distribution data over time and using the maximum recorded value as the representative design parameter is crucial. Further considerations regarding relief system sizing (Section 3.3.) will be addressed for a storage vessel designed for the highest temperature (35 °C). Using an average temperature between reference values for hypothetical winter and summer seasons (5 °C and 35 °C) could lead to misleading conclusions. Importantly, all systems reach a bulk temperature far below the onset temperature, regardless of the modelling theory used. This observation confirms the robustness of the adopted procedure, as both versions of the FKT predict that the maximum temperature in the centre of the tank at steady state is the highest temperature the system can reach. Ensuring that this maximum temperature is well below the onset temperature guarantees that runaway conditions induced by self-heating phenomena related to the thermal decomposition of the stored material are avoided. Additionally, given the intrinsic conservatism of the FKT, which neglects any heat dissipation due to natural convection or primary reactant consumption, the actual bulk steady-state temperature will likely be even lower than the determined value, further enhancing safety.

Comparing the results obtained with the original and expanded FKT reveals significant insights, particularly regarding the δ_{crit} values. In the considered γ interval, ranging from approximately 40 to 51, the δ_{crit} differs by approximately 2.5% compared to the characteristic value of 2.00 predicted by the original FKT for cylindrical geometry. The design outcomes would differ significantly for $\gamma < 10$, where the difference between the predicted δ_{crit} would be approximately 15% or greater. However, for the considered γ interval, storage vessels can be designed using either theory without compromising the quality of the results. Moreover, designing storage equipment with $\delta_{crit} = 2$, regardless of the γ value, results in a system with a lower T_{center} value than predicted by the original FKT, enhancing safety and reliability by increasing the margin between the maximum reachable and onset temperatures. If the storage vessel is designed using the more refined δ_{crit} value from the expanded FKT, the maximum allowable system size would be slightly larger than predicted by the original FKT, with a negligible difference in T_{center}.

An Interesting conclusion from the analysis is the differing stability of the two mixtures considered. The solution containing 50% w/w HA and 1% w/w HH is significantly more stable than the 50% w/w HA solution. This is evident from the $r_{w,crit}$ values obtained with both formulations for the same T_w and geometry. The critical vessel size is almost seven times larger for the solution containing the HA-derived salt than for the one with only HA. The physicochemical properties of the materials can explain this discrepancy. Adding 1% w/w HH increases the activation energy (E_a) and decreases the enthalpy change ($\Delta\widetilde{H}_r$). The higher E_a reduces the likelihood of the decomposition reaction by increasing the energy barrier needed for thermal degradation. The lower $\Delta\widetilde{H}_r$ mitigates the severity of the thermal decomposition, reducing the self-heating of the system. Therefore, with a 50% w/w HA solution containing 1% w/w HH, it is possible to design storage vessels with higher capacity without triggering any self-heating phenomena that could lead to a runaway reaction.

3.3. Sizing of the relief system

For the relief device sizing, a K_d value of 0.975, typical for gas and vapours venting (Crowl and Tipler, 2013), has been adopted. Additionally, a negligible effect of backpressure is assumed ($K_b = 1$), and no rupture disk is placed before the relief valve ($K_c = 1$). The corrective factor for backpressure K_b has been assumed based on a conventional relief valve design (Crowl and Tipler, 2013). For other pressure relief systems, the backpressure and the corresponding K_b value must be quantified (Liptak, 2003). No rupture disk is considered upstream of the relief valve because it is assumed that the stored fluids are not fouling,

Table 3
Output of the storage vessel design method using both the original and the expanded FKT for an aqueous solution of 50 % w/w of HA, and for a 50 % w/w aqueous solution of HA with 1 % w/w of HH, respectively.

50 % w/w HA									
	Original FKT		Expanded FKT						
T_w [K]	$r_{w,crit}$ [m]	T_{center} [K]	γ [-]	δ_{crit} [-]	$\Theta_{max}\|_{\delta_{crit}}$ [-]	$\Theta_{max}\|_{\delta=2}$ [-]	$r_{w,crit}$ [m]	$T_{center}\|_{\delta_{crit}}$ [K]	$T_{center}\|_{\delta=2}$ [K]
278.15	2.93	286.8	44.50	2.045	1.454	1.147	3.20	287.2	285.3
293.15	1.03	302.8	42.23	2.054	1.462	1.140	1.08	303.3	301.1
308.15	0.40	318.8	40.17	2.057	1.462	1.135	0.41	319.4	316.9
50 % w/w HA+1 % w/w HH									
	Original FKT		Expanded FKT						
T_w [K]	$r_{w,crit}$ [m]	T_{center} [K]	γ [-]	δ_{crit} [-]	$\Theta_{max}\|_{\delta_{crit}}$ [-]	$\Theta_{max}\|_{\delta=2}$ [-]	$r_{w,crit}$ [m]	$T_{center}\|_{\delta_{crit}}$ [K]	$T_{center}\|_{\delta=2}$ [K]
278.15	22.65	285.8	50.72	2.044	1.446	1.157	24.65	286.1	284.5
293.15	6.79	301.6	48.12	2.047	1.449	1.152	7.10	302.0	300.2
308.15	2.29	317.5	45.78	2.049	1.452	1.147	2.32	317.9	315.9

eliminating the need for a seal between the equipment and the relief valve (Hellemans, 2009). During the experimental campaign, a gas volume ($V_{gas.test}$) of $8.9 \bullet 10^{-6}\ m^3$ and a total mass $m_{tot} = 1.2\ 10^{-3}\ kg$ were used. The relief pressure (P_{relief}) was set at 1.25 times the operating pressure (P_{op}), with $P_{op} = P_{atm}$ assuming an atmospheric storage tank (Ennis, 2006). The temperature increase rate at relief conditions ($\dot{T}_{relief}$) was conservatively taken as $\dot{T}_{onset}$, and the relief temperature (T_{relief}) was considered to be T_{center}, representing the most critical temperature when the system deviates from standard operating conditions.

Fig. 6 shows the outcome of the relief system sizing using DIERS and standard procedures for a storage vessel designed based on the original FKT with $T_w = 308.15\ K$. In contrast, Fig. 5 implements the expanded version of the FKT, considering $T_{relief} = T_{center}|_{\delta_{crit}}$ and $T_w = 308.15\ K$. The results present the diameter ratio ($d = D_{valve}/D$) as a function of the aspect ratio (H/D) for various void fraction values, ranging from 0.1 to 0.4. The behaviour of the considered HA aqueous solutions (i.e., HA 50% w/w and HA 50% w/w + HH 1% w/w) was also evaluated.

Figs. 5 and 6 show a comparison between the DIERS and standard methodologies for sizing relief devices for both considered HA aqueous solutions and versions of the FKT. The standard method is slightly more conservative than the DIERS in all the cases. If backpressure effects and the presence of relief devices in series are considered, resulting in K_b and K_c coefficients lower than 1, the deviation between the two sizing strategies will further increase. Therefore, the standard algorithm should be preferred for relief device sizing, coupled with DIERS for determining the total mass flow rate ($\dot{W}_{tot}$).

The analysis of the dependence of the diameter ratio ($d = D_{valve}/D$) on the respect ratio (H/D) highlights the connection between vessel geometry and relief device size. For a fixed value of D, a higher H/D ratio means a higher volume (V) and, consequently, a larger amount of stored mass. The greater the quantity of the mixture in the vessel, the more material can undergo thermal degradation, necessitating a larger relief device to vent all the generated gases and vapours during a runaway reaction. Higher H/D ratios can be advantageous in vertical storage tanks, optimising the use of the storage vessel footprint. By keeping D constant and increasing H, the available storage volume can be increased without altering the base area, impacting the plant layout. The higher liquid level must also be considered during relief device sizing to avoid underestimating the required orifice. It is essential to note that the literature does not provide a reference value to assess the maximum safe tank filling ratio. Central norms like API 2350 (ANSI/API, 2020; AS 1940:2017 (AS, 2017) define various liquid heights for safe storage but leave the critical high-level selection to the designer. The critical high level is the highest liquid level in the tank without detrimental impacts, typically not exceeding 95% of this level for the maximum working level.

From Figs. 5 and 6, it is evident that the lower the α_0 (i.e., the higher the liquid level), the higher the d value for a fixed H/D. Both the aspect and the filling ratio must be carefully assessed during the design phase to reliably meet production and operational constraints. A filling ratio corresponding to the critical high liquid level must be chosen to avoid undersizing the relief systems. Figs. 5 and 6 also show that the trend of d versus H/D is consistent for the same HA aqueous solution (i.e., 50% w/w HA or 50% w/w HA added with 1% w/w HH) regardless of the FKT version used. This consistency is because both versions predict almost the same value of $r_{w,crit}$ and T_{center} for the considered γ value.

Another significant observation from Figs. 5 and 6 is the impact of larger storage tanks on the relief system. According to Eqs. (12)–(14), there is a linear relationship between V, $\dot{W}_{tot}$ and the orifice area. Although the mixture containing 1% w/w HH is more stable and can be handled safely in larger equipment, the increased storage volume presents a significant drawback. A larger V means more stored material and, consequently, a higher flow rate of decomposition products to the vent, necessitating a more substantial overpressure relief system. For large H/D values, especially for the 50% w/w HA added with 1% w/w HH solution, the relief system may have oversized orifice areas that are impractical to implement. This scenario is noted by (Lees, 2012), who states that the vent area can be so large that it cannot fit on some vessels, particularly when chemical reactions occur inside the system. In such cases, pressure relief systems are not a practical option, underscoring the need for intrinsically safe design processes and equipment to enhance industrial plant reliability and mitigate risks associated with large storage vessels.

4. Conclusions

Storage vessels are critical industrial equipment, often containing large quantities of materials. Ensuring the safety of these stored materials is essential during the design process (Bassani et al., 2023), especially for thermally unstable compounds. This work presents a methodology to determine the size of an intrinsically safe system capable of preventing runaway conditions triggered by exothermic decomposition reactions. A stability diagram was developed by selecting key design variables to saturate the system's degrees of freedom and verify the consistency of numerical results. Additionally, active protection measures such as relief systems can be implemented to vent gaseous and vapour decomposition products, further enhancing plant safety.

The proposed methodology was tested on two unstable mixtures: aqueous solutions of 50% w/w HA and 50% w/w HA with 1% w/w HH. Preliminary screening indicated that the solution containing 50% w/w HA with 1% w/w HH exhibited a lower thermal degradation tendency than the solution with only 50 % w/w HA. Due to the higher stability of the 50% w/w HA + 1% w/w HH mixture, results showed the possibility of designing a storage vessel with a larger characteristic dimension (i.e., vessel radius) compared to the 50% w/w HA solution while still avoiding runaway phenomena induced by self-heating. Thus, adding 1 %w HH to a 50 %w HA aqueous solution not only enhances the reli-

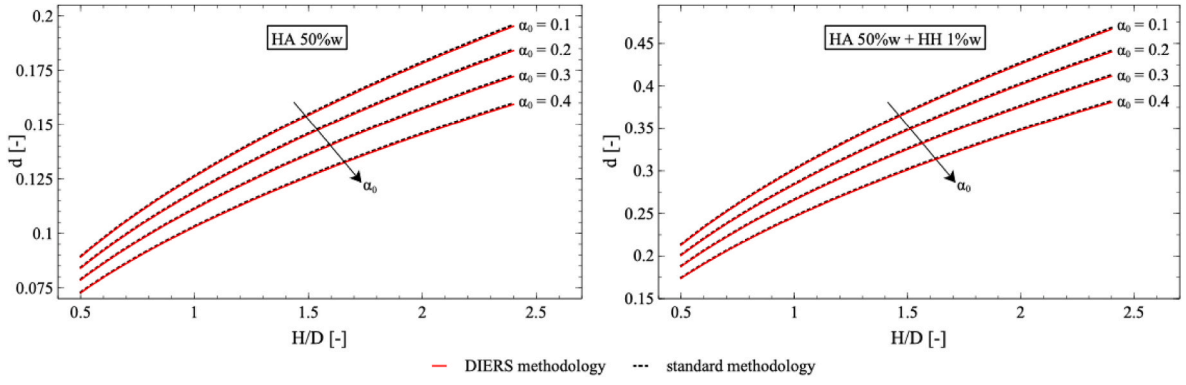

Fig. 5. Relief devices sizing outcomes using the expanded FKT for various filling ratios.

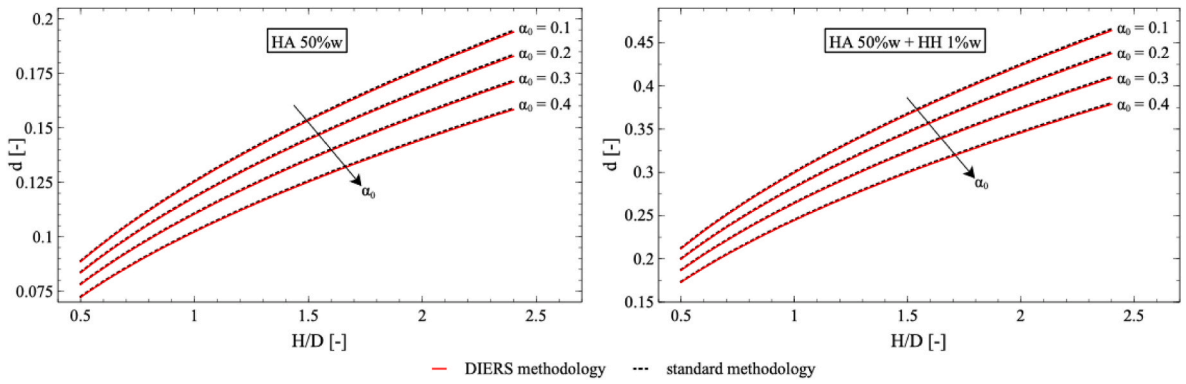

Fig. 6. Relief devices sizing outcomes using the original FKT for various filling ratios.

ability of the chemical plant by reducing the probability and severity of potential decomposition reactions but also allows for larger storage vessels without compromising process safety. The presented procedure employs a $\delta - \gamma$ stability diagram coupled with a $\Theta_{max} - \gamma$ map as versatile tools for designing cylindrical storage vessels handling hazardous materials prone to thermal degradation.

Ultimately, the design of relief systems must be approached critically and carefully in industrial settings where runaway conditions can occur. This highlights the importance of intrinsically safe design for storage equipment, demonstrating that active protection measures may not be feasible in some cases when large quantities of chemicals and severe side phenomena are involved.

CRediT authorship contribution statement

Giuseppe Andriani: Writing – original draft, Methodology, Investigation, Formal analysis, Data curation, Conceptualization. **Paolo Mocellin:** Writing – review & editing, Writing – original draft, Supervision, Project administration, Investigation, Funding acquisition, Conceptualization. **Gianmaria Pio:** Writing – review & editing, Validation, Methodology, Data curation. **Chiara Vianello:** Writing – review & editing, Resources, Project administration, Funding acquisition. **Ernesto Salzano:** Writing – review & editing, Supervision, Resources, Project administration.

Declaration of competing interest

The authors have declared no conflict of interest.

Data availability

Data will be made available on request.

References

Andriani, Giuseppe, De Liso, B.A., Pio, G., Salzano, E., 2024a. Design of sustainable reactor based on key performance indicators. Chem. Eng. Sci. 285, 119591. https://doi.org/10.1016/j.ces.2023.119591.

Andriani, G., Mocellin, P., Pio, G., Salzano, E., Vianello, C., 2024b. Hydroxylamine vs. Hydrogen peroxide: a comparative study on storage stability. Chem Eng Trans 111, 277–282. https://doi.org/10.3303/CET24111047.

Andriani, Giuseppe, Pio, G., Salzano, E., Vianello, C., Mocellin, P., 2024c. Evaluating the thermal stability of chemicals and systems: a review. Can. J. Chem. Eng. https://doi.org/10.1002/cjce.25422.

Andriani, Giuseppe, Pio, G., Vianello, C., Mocellin, P., Salzano, E., 2024d. Safety parameters and stability diagram of hydroxylamine hydrochloride and sulphate. Chem. Eng. J. 148894. https://doi.org/10.1016/j.cej.2024.148894.

ANSI/API, 2007. Pressure-relieving and Depressuring Systems: ANSI/API, 521, fifth ed. ANSI/API.

ANSI/API, 2020. Overfill Prevention for Storage Tanks in Petroleum Facilities: ANSI/API Standard 2350, fifth ed. ANSI/API.

API, 1998. Venting Atmospheric and Low-Pressure Storage Tanks: API 2000, fifth ed. API.

ARIA database [WWW Document], n.d. URL https://www.aria.developpement-durable.gouv.fr/the-barpi/the-aria-database/?lang=en.

AS, 2017. The Storage and Handling of Flammable and Combustible Liquids: AS 1940, seventh ed. Standards Australia.

Babrauskas, V., 2003. Ignition Handbook: Principles and Applications to Fire Safety Engineering, Fire Investigation, Risk Management and Forensic Science.

Balakrishnan, E., Wake, G.C., 1996. Critical values for some non-class A geometries in thermal ignition theory. Mathl. Comput. Modelling 24. https://doi.org/10.1016/0895-7177(96)00133-1.

Barton, J.A., Nolan, P.F., 1991. Incidents in the chemical industries due to thermal runaways chemical reactions. IChemE SYMPOSIUM SERIES No. 115.

Bassani, A., Vianello, C., Mocellin, P., Dell'Angelo, A., Spigno, G., Fabiano, B., Maschio, G., Manenti, F., 2023. Aprioristic integration of process operations and risk analysis: definition of the weighted F&EI-Based concept and application to AG2S technology. Ind. Eng. Chem. Res. 62, 500–510. https://doi.org/10.1021/acs.iecr.2c02289.

Boddington, T., Feng, C.-G., Gray, P., 1983. Thermal explosions, criticality and the disappearance of criticality in systems with distributed temperatures. I. Arbitrary biot number and general reaction-rate laws. Source: Proc. Roy. Soc. Lond. Math. Phys. Sci. 390, 247–264. https://doi.org/10.1098/rspa.1983.0130.

Campbell, A.N., 2015. The effect of external heat transfer on thermal explosion in a spherical vessel with natural convection. Phys. Chem. Chem. Phys. 17, 16894–16906. https://doi.org/10.1039/c5cp02302e.

Chambré, P.L., 1952. On the solution of the Poisson-Boltzmann equation with application to the theory of thermal explosions. J. Chem. Phys. 20, 1795–1797. https://doi.org/10.1063/1.1700291.

Crowl, D.A., Tipler, S.A., 2013. Sizing pressure-relief devices. Chem. Eng. Prog. 109, 68–76.

CSB database [WWW Document], n.d. URL https://www.csb.gov/investigations/completed-investigations/?F_AccidentTypeId=1269&pg=1.

Dakkoune, A., Vernières-Hassimi, L., Leveneur, S., Lefebvre, D., Estel, L., 2019. Analysis of thermal runaway events in French chemical industry. J. Loss Prev. Process. Ind. https://doi.org/10.1016/j.jlp.2019.103938.

Deng, J., Zhao, J., Zhang, Y., Huang, A., Liu, X., Zhai, X., Wang, C., 2016. Thermal analysis of spontaneous combustion behavior of partially oxidized coal. Process Saf. Environ. Protect. https://doi.org/10.1016/j.psep.2016.09.007.

Eckerman, I., 2005. The Bhopal gas leak: analyses of causes and consequences by three different models. J. Loss Prev. Process. Ind. 18, 213–217. https://doi.org/10.1016/j.jlp.2005.07.007.

Emerson, 2012. Pressure Relief Valve Engineering Handbook, first ed. Emerson.

Ennis, T., 2006. Pressure relief considerations for low-pressure (atmospheric) storage tanks. IChemE Symposium Series 1–13.

Fabiano, B., Vianello, C., Reverberi, A.P., Lunghi, E., Maschio, G., 2017. A perspective on Seveso accident based on cause-consequences analysis by three different methods. J. Loss Prev. Process. Ind. 49, 18–35. https://doi.org/10.1016/j.jlp.2017.01.021.

Fisher, H.G., Forrest, H.S., Grossel, S.S., Huff, J.E., Muller, A.R., Noronha, J.A., Shaw, D. A., Tilley, B.J., 1992. Emergency Relief System Design Using DIERS Technology: the Design Institute for Emergency Relief Systems (DIERS) Project Manual, first ed. American Institute of Chemical Engineers.

Frank-Kamenetskii, D.A., 1955. Diffusion and Heat Exchange in Chemical Kinetic.

Gangloff, J.J., Kast, J., Morrison, G., Marcinkoski, J., 2017. Design space assessment of hydrogen storage onboard medium and heavy duty fuel cell electric trucks. Journal of Electrochemical Energy Conversion and Storage 14. https://doi.org/10.1115/1.4036508.

Geyer, W.B., Wisuri, J., 2000. Handbook of Storage Tank Systemns: Codes, Regulations, and Designs, first ed. Marcel Dekker.

Godoy, L.A., 2016. Buckling of vertical oil storage steel tanks: review of static buckling studies. Thin-Walled Struct. https://doi.org/10.1016/j.tws.2016.01.026.

Green, D.W., Southard, M.Z., 2019. Perry's Chemical Engineers' Handbook, ninth ed. McGraw-Hill Education.

Guo, W., Lim, C.J., Bi, X., Sokhansanj, S., Melin, S., 2013. Determination of effective thermal conductivity and specific heat capacity of wood pellets. Fuel 347–355. https://doi.org/10.1016/j.fuel.2012.08.037.

Hellemans, M., 2009. The Safety Relief Valve Handbook: Design and Use of Process Safety Valves to ASME and International Codes and Standards, first ed. Elsevier.
Ho, T.C., Duh, Y.S., Chen, J.R., 1998. Case studies of incidents in runaway reactions and emergency relief. Process Saf. Prog. 17, 259–262. https://doi.org/10.1002/prs.680170406.
Jain, P., Pasman, H.J., Waldram, S.P., Rogers, W.J., Mannan, M.S., 2017. Did we learn about risk control since Seveso? Yes, we surely did, but is it enough? An historical brief and problem analysis. J. Loss Prev. Process. Ind. 49, 5–17. https://doi.org/10.1016/j.jlp.2016.09.023.
Juncheng, J., Dan, W., Lei, N., Gang, F., Yong, P., 2020. Inherent thermal runaway hazard evaluation method of chemical process based on fire and explosion index. J. Loss Prev. Process. Ind. 64. https://doi.org/10.1016/j.jlp.2020.104093.
Kletz, T.A., 2003. Inherently safer design - its scope and future. Process Saf Environ Prot 81, 401–405. https://doi.org/10.1205/095758203770866566.
Kletz, T., Amyotte, P., 2010. Process Plants: A Handbook for Inherently Safer Design, second ed. CRC Press - Taylor & Francis Group.
Lazarovici, A., Volpert, V., Merkin, J.H., 2005. Steady states, oscillations and heat explosion in a combustion problem with convection. Eur. J. Mech. B Fluid 24, 189–203. https://doi.org/10.1016/j.euromechflu.2004.06.007.
Lees, F., 2012. Lees' Loss Prevention in the Process Industries: Hazard Identification, Assessment and Control, fourth ed. Butterworth-Heinemann.
Lengyel, I., West, D.H., 2018. Numerical bifurcation analysis of large-scale detailed kinetics mechanisms. Curr Opin Chem Eng 21, 41–47. https://doi.org/10.1016/j.coche.2018.02.013.
Liptak, B.G., 2003. Instrument Engineers' Handbook - Volume 1: Process Measurement and Analysis, fourth ed. CRC Press.
Mocellin, P., De Tommaso, J., Vianello, C., Maschio, G., Saulnier-Bellemare, T., Virla, L. D., Patience, G.S., 2022. Experimental methods in chemical engineering: hazard and operability analysis—HAZOP. Can. J. Chem. Eng. 100, 3450–3469. https://doi.org/10.1002/cjce.24520.
Myers, P.E., 1997. Aboveground Storage Tanks, first ed. McGraw-Hill.
Novozhilov, V., 2017. Effects of initial and boundary conditions on thermal explosion development. In: AIP Conference Proceedings. American Institute of Physics Inc. https://doi.org/10.1063/1.4972706.
Ozawa, T., 2000. Thermal analysis — review and prospect. Thermochim. Acta 355, 35–42. https://doi.org/10.1016/S0040-6031(00)00435-4.
Ozbek, H., Phillips, S.L., 1980. Thermal conductivity of aqueous sodium chloride solutions from 20°C to 330°C. J. Chem. Eng. Data 25, 263–267. https://doi.org/10.1021/je60086a001.
Pio, G., Salzano, E., 2020. Gas-phase thermal explosions in catalytic direct oxidation of alkenes. J. Loss Prev. Process. Ind. 65. https://doi.org/10.1016/j.jlp.2020.104097.
Pio, G., Mocellin, P., Vianello, C., Salzano, E., 2021. A detailed kinetic model for the thermal decomposition of hydroxylamine. J. Hazard Mater. 416. https://doi.org/10.1016/j.jhazmat.2021.125641.
Restuccia, F., Ptak, N., Rein, G., 2017. Self-heating behavior and ignition of shale rock. Combust. Flame 176, 213–219. https://doi.org/10.1016/j.combustflame.2016.09.025.
Saada, R., Patel, D., Saha, B., 2015. Causes and consequences of thermal runaway incidents - will they ever be avoided? Process Saf. Environ. Protect. 97, 109–115. https://doi.org/10.1016/j.psep.2015.02.005.
Shanley, E.S., 1953. Self-healing of hydrogen peroxide storage vessels. Ind. Eng. Chem. 45, 1520–1524. https://doi.org/10.1021/ie50523a044.
Singh, J., 1994. Vent sizing for gas-generating runaway reactions. J. Loss Prev. Process. Ind. 7, 481–491. https://doi.org/10.1016/0950-4230(94)80006-5.
Strozzi, F., Zaldıvar′, J.M.Z., Kronberg, A.E., Westerterp, K.R., 1999. On-line runaway detection in batch reactors using chaos theory techniques. AIChE J. 45, 2429–2443. https://doi.org/10.1002/aic.690451116.
Varma, Arvind, Morbidelli, Massimo, Wu, Hua, 1999. Parametric sensitivity. In: Chemical Systems, first ed. Cambridge University Press.
Vianello, C., Salzano, E., Maschio, G., 2015. Safety parameters and preliminary decomposition kinetic of organo-peroxy acids in aqueous phase. Chem Eng Trans 43, 2371–2376. https://doi.org/10.3303/CET1543396.
Vianello, C., Salzano, E., Maschio, G., 2016. Kinetics and safety analysis of peracetic acid. Chem Eng Trans 48, 559–564. https://doi.org/10.3303/CET1648094.
Vianello, C., Salzano, E., Broccanello, A., Manzardo, A., Maschio, G., 2018a. Runaway reaction for the esterification of acetic anhydride with methanol catalyzed by sulfuric acid. Ind. Eng. Chem. Res. 57, 4195–4202. https://doi.org/10.1021/acs.iecr.7b05160.
Vianello, C., Salzano, E., Maschio, G., 2018b. Thermal behaviour of Peracetic Acid for the epoxydation of vegetable oils in the presence of catalyst. Process Saf. Environ. Protect. 116, 718–726. https://doi.org/10.1016/j.psep.2018.03.030.
Wang, Q., Rogers, W.J., Mannan, M.S., 2009. Thermal risk assessment and rankings for reaction hazards in process safety. J. Therm. Anal. Calorim. 98, 225–233. https://doi.org/10.1007/s10973-009-0135-z.
Yang, M., Khan, F., Amyotte, P., 2015. Operational risk assessment: a case of the Bhopal disaster. Process Saf. Environ. Protect. 97, 70–79. https://doi.org/10.1016/j.psep.2015.06.001.
Zhang, H., Bai, M., Wang, X., Gai, J., Shu, C.M., Roy, N., Liu, Y., 2021. Thermal runaway incidents-a serious cause of concern: an analysis of runaway incidents in China. Process Saf. Environ. Protect. 155, 277–286. https://doi.org/10.1016/j.psep.2021.09.027.